# Infrared absorption of H⁻ and D⁻ in the alkaline-earth fluorides

# Infrared absorption of H⁻ and D⁻ in the alkaline-earth fluorides

**Glynn D Jones[1,3], James J Y Sung[1], Timothy Hume[1], Liem Suk Ing[1], Ian V Bradley[2] and Jon-Paul R Wells[2]**

[1] Department of Physics and Astronomy, University of Canterbury, PB 4800, Christchurch, 8020, New Zealand
[2] FELIX free-electron laser facility, FOM—Institute for Plasmaphysics—'Rijnhuizen', PO Box 1207, 3430 BE Nieuwegein, The Netherlands

E-mail: g.jones@phys.canterbury.ac.nz

**Abstract**
A revisit is made to the infrared absorption spectra of H⁻ and D⁻ local modes in the alkaline-earth fluorides. New data on the intensity ratios of the various harmonic lines, observation of a fourth harmonic for H⁻ in $CaF_2$ and revised values for the anharmonic potential well constants are presented, together with temperature-dependent linewidths measured for the H⁻ third-harmonic lines.

## 1. Introduction

Thirty-five years ago, the infrared absorption spectra of the localized vibrations of H⁻ and D⁻ ions in the alkaline-earth fluorides were reported [1]. Experimental investigations of the spectroscopy of these ions were established by Bill Hayes, with Roger Elliott providing theoretical insight.

This paper readdresses these spectroscopic systems and presents additional data. With the advent of FTIR techniques and curve-fitting routines, the original results can be confirmed, modified and supplemented with relative ease. We fill out the data on several aspects:

- The H⁻ and D⁻ third harmonics for both $SrF_2$ and $BaF_2$ are reported.
- Anharmonic potential analyses are carried out for H⁻ and D⁻ for all three hosts.
- A set of the measured relative intensities of all of the second- and third-harmonic lines is presented.
- One of the two expected fourth harmonics of H⁻ in $CaF_2$ is observed, while the other fourth harmonic remains elusive.
- The H⁻ third-harmonic lines are found to broaden rapidly with temperature through one-phonon processes.

[3] Author to whom any correspondence should be addressed. Telephone: +64 3 364 2563; fax: +64 3 364 2469.

H$^-$ and D$^-$ ions have proved to be excellent spectroscopic probes of ionic fluoride crystals. The study of H$^-$ and D$^-$ in the alkaline-earth fluorides started by Bill Hayes in 1962 developed into infrared studies of H$^-$ and D$^-$ charge-compensated trivalent rare-earth ions [2–4], with varied manifestations of the electron–phonon interaction between the rare-earth and hydrogenic ions [5, 6].

Several hydrogenic rare-earth centres have been investigated optically for many rare-earth ions [7–9] by the powerful techniques of laser selective excitation, first applied to rare-earth-doped CaF$_2$ by John Wright and his co-workers [10]. Light-induced migration of the hydrogenic ions between equivalent and inequivalent sites was an unexpected aspect arising from these laser studies [11, 12].

The dynamics of the original H$^-$ and D$^-$ system has been followed up with the advent of high-power tunable infrared lasers [13–16], with recent detailed studies from the free-electron laser facility (FELIX) in Holland [16]. The latest results from FELIX are reported in another paper in this Special Issue.

## 2. Experimental procedure

The CaF$_2$, SrF$_2$ and BaF$_2$ crystals were all offcuts purchased from Optovac Incorporated. H$^-$ or D$^-$ ions are introduced by heating the crystals in hydrogen or deuterium gas at up to 2/3 atmosphere with the crystals in contact with molten aluminium metal at temperatures between 740 and 860 °C, for periods ranging from 5 min to 120 h [17]. Of the three alkaline-earth fluoride crystals, BaF$_2$ is the most ready to take up H$^-$ while CaF$_2$ is the least. Infrared absorption spectra were measured at either 0.25 or 0.1 cm$^{-1}$ resolution with a Bio-Rad FTS-40 Fourier transform infrared spectrometer. Samples were mounted on a copper holder cooled by thermal contact with the 10 K cold stage of a Cryosystem CTS LTS 0.1 closed-cycle helium cryostat. Temperature dependence studies were carried out by raising the temperature of the crystals in 30 K steps, with a heater in a temperature-control loop giving set temperatures to within 1 K.

Specialized curve-fitting routines were used to determine the frequencies, linewidths and relative intensities of the infrared absorption lines of the H$^-$ and D$^-$ local modes, with these lines having profiles close to Lorentzian.

For measurement of the intense fundamentals of H$^-$ and D$^-$, very lightly doped crystals were needed. H$^-$ lines of low intensity and of the narrowest width could obtained for deuterated crystals where the traces of about 2% hydrogen present were sufficient to give very weak and narrow H$^-$ lines. Likewise, weak narrow D$^-$ lines could be obtained by using a 4:1 hydrogen-to-deuterium atmosphere, where competition between the hydrogen and deuterium reduced the amount of D$^-$ introduced.

The lower-energy third-harmonic line of H$^-$ in BaF$_2$ occurred among the vibrational–rotational lines of atmospheric carbon dioxide, which were ratioed out. Crystals of up to 2 cm thickness were needed to reveal the broad third-harmonic lines of D$^-$ in the three hosts, with SrF$_2$ having the weakest harmonic lines of the three. As the D$^-$ second- and third-harmonic lines occur among atmospheric water lines, ratioing of their spectra with background spectra of closely similar atmospheric water absorption was necessary to clearly reveal the broader-profile third-harmonic lines.

For the search for the two expected fourth harmonics of H$^-$ in CaF$_2$, use was made of a series of crystals hydrogenated some years ago in a high-pressure (up to 70 bar) hydrogen atmosphere in a stainless steel vessel, with a small internal furnace. All of the H$^-$ local mode lines of these crystals were an order of magnitude more intense than those of conventionally hydrogenated crystals, but these stronger lines were broader than usual, with the third-harmonic

H$^-$ lines not quite reaching the 100% absorption needed to ensure observing weaker higher-harmonic transitions. Multiple crystals totalling a thickness of 5 cm revealed one of the expected fourth-harmonic lines of H$^-$ in CaF$_2$, while the other fourth-harmonic line eluded detection. Observation of the corresponding fourth-harmonic lines of H$^-$ for SrF$_2$ and BaF$_2$ would need prior identification of the various vibrational lines of extraneous OH$^-$ ions that may occur in the same spectral region as any expected H$^-$ fourth-harmonic line.

Relative intensities were measured on appropriately hydrogenated and deuterated samples of optimum thicknesses that give less than 100% absorption for the peak of the stronger line yet allow the recording of the weaker line at good intensity. For the D$^-$ lines of SrF$_2$, the intensity ratios approach 100:1 and optimal doping was critical. Some of the earlier results reported in 1965 relied on uniformity of hydrogenation of the sample with the weaker line measured for the full thickness and the stronger line measured for a thin slice from this. For other earlier results, the room temperature profile of the stronger line was compared with the 20 K profile of the weaker line, which required knowledge of the intensity dependence of the stronger line on temperature to derive the desired intensity ratios. The advent of curve-fitting routines and the wide dynamic range of FTIR spectroscopy avoids these approximations.

## 3. Anharmonic potential well analysis for H$^-$ and D$^-$ local modes

For H$^-$ and D$^-$ ions in pure CaF$_2$, SrF$_2$ and BaF$_2$, the hydrogenic ions are located at the F$^-$ sites of tetrahedral (T$_d$) symmetry [1]. One fundamental, one second-harmonic and two third-harmonic transitions are observed, whose recently measured frequencies and linewidths at 10 K are listed in table 1.

For the light hydrogenic ions, the local modes are strongly localized and to a good approximation the rest of the lattice may be taken as static. The potential well appropriate for hydrogenic ions in sites of tetrahedral T$_d$ symmetry has the following form for terms of fourth order in the $(x, y, z)$ ion displacements:

$$V = \hbar\Omega(x^2 + y^2 + z^2) + Bxyz + C_1(x^4 + y^4 + z^4) + C_2(x^2y^2 + y^2z^2 + z^2x^2).$$

The energies $E_{n_1,n_2,n_3}$ of the various levels are

$$E_{n_1,n_2,n_3} = \nu\hbar\Omega + (\mu_1 C_1 + \mu_2 C_2)\alpha^4 - \lambda B^2\alpha^6/3\hbar\omega$$

where the values of $\mu_1$, $\mu_2$ and $\lambda$ are reproduced in table 2 of [1] supplemented by inclusion of results for the $\nu = 4$ levels needed for confirming any observation of fourth-harmonic lines. The eigenfunctions are listed as $|n_1, n_2, n_3\rangle$ where $n_1 + n_2 + n_3 = \nu$.

The four measured local mode frequencies of H$^-$ or D$^-$ for each host are sufficient to determine $\Omega$, $B$, $C_1$ and $C_2$ for each and these constants are listed in table 3. The uncertainties in the anharmonic constants can be large because of the sensitivity of the values to the small anharmonic shifts. A measure of the sensitivity of the quartic anharmonic constants $C_1$ and $C_2$ to the exact values of the measured frequencies is shown in their greatly revised values for the remeasured data, which are minimally shifted from the original 20 K data.

The derived anharmonic constants for SrF$_2$ and BaF$_2$ were reported in [18] and form a consistent set, giving confidence in their values. Again, small changes in the spectroscopic data from them lead to significant changes in the quartic anharmonic constants.

To obtain the anharmonic constants more accurately would require precise remeasurement of all local mode lines for lightly doped crystals immersed in liquid helium. The weakness of all third-harmonic lines requires measurement of thick samples, while the fundamentals are only measurable for thin samples, making sample variation a remaining factor affecting the precision of measurements of the small anharmonic shifts.

**Table 1.** Peak positions (cm$^{-1}$) and linewidths (cm$^{-1}$) at 10 K of the localized vibrational modes of H$^-$ and D$^-$ ions in the alkaline-earth fluorides.

| Crystal | Line | Peak position | Width |
|---|---|---|---|
| CaF$_2$:H$^-$ | Fundamental | 965.3 | 0.27 |
| | Second harmonic | 1920.3 | 0.44 |
| | Third harmonic | 2826.0 | 0.6 |
| | Third harmonic | 2913.1 | 2.9 |
| CaF$_2$:D$^-$ | Fundamental | 694.6 | 1.6 |
| | Second harmonic | 1384.5 | 3.9 |
| | Third harmonic | 2048.6 | 7.1 |
| | Third harmonic | 2093.3 | 5.7 |
| SrF$_2$:H$^-$ | Fundamental | 892.7 | 0.25 |
| | Second harmonic | 1775.0 | 0.47 |
| | Third harmonic | 2605.7 | 0.5 |
| | Third harmonic | 2695.7 | 4.8 |
| SrF$_2$:D$^-$ | Fundamental | 640.1 | 0.8 |
| | Second harmonic | 1275.6 | 1.6 |
| | Third harmonic | 1884.1 | 3.2 |
| | Third harmonic | 1930.3 | 2.4 |
| BaF$_2$:H$^-$ | Fundamental | 802.0 | 0.21 |
| | Second harmonic | 1592.5 | 0.6 |
| | Third harmonic | 2329.0 | 0.5 |
| | Third harmonic | 2425.4 | 7.7 |
| BaF$_2$:D$^-$ | Fundamental | 575.4 | 0.85 |
| | Second harmonic | 1146.1 | 2.2 |
| | Third harmonic | 1687.8 | 2.6 |
| | Third harmonic | 1736.3 | 2.5 |

The consistency of the present values for the three hosts gives some confidence in the revised values for H$^-$ in CaF$_2$, which can now account for the observed intensity ratio of the two H$^-$ third-harmonic lines of CaF$_2$.

The D$^-$ data were separately fitted and gave slightly larger values for the anharmonic constants (table 3). The approximation of a single particle vibrating in a potential well is less satisfactory for D$^-$, where the localized mode will extend a little. The quartic constants $C_1$ and $C_2$ determined for D$^-$ differ noticeably from those for H$^-$ and do not account for the observed intensity ratios of the two D$^-$ third-harmonic lines.

## 4. Observation of the $\Gamma_1$ and $\Gamma_3$ second-harmonic transitions

The energies of all the anharmonic levels predicted from the anharmonic constants of table 3 are listed in table 4. The energies of the $\Gamma_1$ and $\Gamma_3$ second-harmonic levels have been determined by several techniques including uniaxial stress measurements [18], Raman scattering [19, 20] and excitation of transitions from the $\Gamma_5$ fundamental in spectrally resolved free-induction-decay (FID) experiments [15].

The spectrally resolved FID vibrational ladder-climbing experiments were performed at the FELIX free-electron laser facility employing a non-collinear degenerate four-wave

**Table 2.** Positions and forms of the lower vibrational levels of H$^-$ and D$^-$ ions in the alkaline-earth fluorides.

| $\nu$ | Irrep | Wavefunction | $\mu_1$ | $\mu_2$ | $\lambda$ |
|---|---|---|---|---|---|
| 0 | $\Gamma_1$ | $|000\rangle$ | 9 | 3 | 1 |
| 1 | $\Gamma_5$ | $|100\rangle$ | 21 | 7 | 5 |
| 2 | $\Gamma_1$ | $(1/\sqrt{3})[|200\rangle + |020\rangle + |002\rangle]$ | 45 | 15 | 21 |
| 2 | $\Gamma_3$ | $(1/\sqrt{2})[|200\rangle - |020\rangle]$ | 45 | 9 | 3 |
| 2 | $\Gamma_5$ | $|011\rangle$ | 33 | 15 | 13 |
| 3 | $\Gamma_1$ | $|111\rangle$ | 45 | 27 | 25 |
| 3 | $\Gamma_4$ | $(1/\sqrt{2})[|102\rangle - |120\rangle]$ | 57 | 21 | 15 |
| 3 | $\Gamma_5^{(1)}$ $\Gamma_5^{(2)}$ | $(1/\sqrt{2})[|102\rangle + |120\rangle]$ $|300\rangle$ | $\begin{pmatrix} 57 & 0 \\ 0 & 81 \end{pmatrix}$ | $\begin{pmatrix} 25 & 2\sqrt{6} \\ 2\sqrt{6} & 15 \end{pmatrix}$ | $\begin{pmatrix} 27 & 6\sqrt{6} \\ 6\sqrt{6} & 13 \end{pmatrix}$ |
| 4 | $\Gamma_1^{(1)}$ $\Gamma_1^{(2)}$ | $(1/\sqrt{3})[|400\rangle + |040\rangle + |004\rangle]$ $(1/\sqrt{3})[|022\rangle + |202\rangle + |220\rangle]$ | $\begin{pmatrix} 149 & 0 \\ 0 & 81 \end{pmatrix}$ | $\begin{pmatrix} 17 & 4\sqrt{6} \\ 4\sqrt{6} & 39 \end{pmatrix}$ | $\begin{pmatrix} 17 & 12\sqrt{6} \\ 12\sqrt{6} & 45 \end{pmatrix}$ |
| 4 | $\Gamma_3^{(1)}$ $\Gamma_3^{(2)}$ | $(1/\sqrt{2})[|400\rangle - |040\rangle]$ $(1/\sqrt{2})[|202\rangle - |022\rangle]$ | $\begin{pmatrix} 149 & 0 \\ 0 & 81 \end{pmatrix}$ | $\begin{pmatrix} 17 & 2\sqrt{6} \\ 2\sqrt{6} & 31 \end{pmatrix}$ | $\begin{pmatrix} 17 & 6\sqrt{6} \\ 6\sqrt{6} & 27 \end{pmatrix}$ |
| 4 | $\Gamma_4$ | $(1/\sqrt{2})[|301\rangle - |103\rangle]$ | 93 | 25 | 11 |
| 4 | $\Gamma_5^{(1)}$ $\Gamma_5^{(2)}$ | $(1/\sqrt{2})[|301\rangle + |103\rangle]$ $|121\rangle$ | $\begin{pmatrix} 93 & 0 \\ 0 & 69 \end{pmatrix}$ | $\begin{pmatrix} 37 & 2\sqrt{6} \\ 2\sqrt{6} & 39 \end{pmatrix}$ | $\begin{pmatrix} 47 & 6\sqrt{6} \\ 6\sqrt{6} & 37 \end{pmatrix}$ |

**Table 3.** The constants $\Omega$, $B$, $C_1$ and $C_2$ (with their units in parentheses) for an anharmonic potential well determined from an exact fit of the four $\Gamma_5$ energy levels of the anharmonic potential well to the four $\Gamma_1 \rightarrow \Gamma_5$ local mode transitions measured at 10 K for H$^-$ and D$^-$ local modes in the alkaline-earth fluorides.

| | H$^-$ | | | D$^-$ | | |
|---|---|---|---|---|---|---|
| | CaF$_2$ | SrF$_2$ | BaF$_2$ | CaF$_2$ | SrF$_2$ | BaF$_2$ |
| $\Omega$ (cm$^{-1}$) | 979.5 | 907.3 | 817.5 | 701.3 | 646.7 | 582.4 |
| $B$ ($10^{11}$ J m$^{-3}$) | 8.21 | 7.21 | 6.01 | 8.85 | 7.69 | 6.44 |
| $C_1$ ($10^{20}$ J m$^{-4}$) | $-2.19$ | $-2.03$ | $-1.60$ | $-2.36$ | $-1.99$ | $-1.87$ |
| $C_2$ ($10^{20}$ J m$^{-4}$) | 2.16 | 2.54 | 1.44 | 5.86 | 6.18 | 5.85 |

mixing geometry as used for two-pulse photon-echo measurements. For the essentially homogeneously broadened H$^-$ local mode lines, the signal observed in the $|2k_2 - k_1|$ direction corresponds to free-induction (or free-polarization) decay only. The integrated transient signal observed as a function of the delay between the two pulses was observed to have quantum beats in negative time as a consequence of interference between the multiple coherently excited $\nu = 2$ vibrational states. By dispersing this signal in a spectrometer for a fixed time delay, the

**Table 4.** Calculated energies of the vibrational levels of H⁻ and D⁻ ions in the alkaline-earth fluorides for the values of the anharmonic constants of table 3, which exactly fit the four $\Gamma_5$ levels.

| | | | H⁻ | | | D⁻ | |
|---|---|---|---|---|---|---|---|
| $\nu$ | Symmetry | $CaF_2$ | $SrF_2$ | $BaF_2$ | $CaF_2$ | $SrF_2$ | $BaF_2$ |
| 1 | $\Gamma_5$ | 965.3 | 892.7 | 802.0 | 694.6 | 640.1 | 575.4 |
| 2 | $\Gamma_1$ | 1893.3 | 1746.6 | 1563.0 | 1369.7 | 1260.2 | 1129.5 |
| 2 | $\Gamma_3$ | 1943.5 | 1798.6 | 1618.4 | 1395.9 | 1287.2 | 1158.0 |
| 2 | $\Gamma_5$ | 1920.3 | 1775.0 | 1592.5 | 1384.5 | 1275.6 | 1146.1 |
| 3 | $\Gamma_5^{(2)}$ | 2826.0 | 2605.7 | 2329.0 | 2048.2 | 1884.1 | 1687.8 |
| 3 | $\Gamma_1$ | 2865.0 | 2646.9 | 2371.4 | 2069.7 | 1906.5 | 1712.1 |
| 3 | $\Gamma_4$ | 2888.2 | 2670.5 | 2397.4 | 2081.1 | 1918.1 | 1723.9 |
| 3 | $\Gamma_5^{(1)}$ | 2913.1 | 2695.7 | 2425.3 | 2093.2 | 1930.3 | 1736.4 |

corresponding transition frequencies can be measured. Figure 1 shows the measured spectra for $CaF_2$:H⁻ and $BaF_2$:H⁻.

The observations of the various techniques are collected together in table 5 and are in agreement with each other and with the predicted values of table 4.

**Table 5.** Measured $\nu = 2$ energy levels for H⁻ and D⁻ local modes in the alkaline-earth fluorides obtained from the references cited.

| | | | H⁻ | | | | | D⁻ | |
|---|---|---|---|---|---|---|---|---|---|
| | | $CaF_2$ | | $SrF_2$ | | $BaF_2$ | $CaF_2$ | $SrF_2$ | $BaF_2$ |
| Reference: | [18] | [20] | [16] | [20] | [19] | (New) | [20] | [20] | [19] |
| $\Gamma_1$ | 1894.0 | 1891.5 | $1893 \pm 2$ | 1745.0 | 1566 | $1562.7 \pm 0.2$ | 1369.2 | 1259.1 | 1133 |
| $\Gamma_5$ | 1919.8 | 1919.0 | $1920.1 \pm 0.3$ | 1774.6 | 1597 | $1593.4 \pm 0.5$ | 1383.7 | 1275.3 | 1150 |
| $\Gamma_3$ | 1945.0 | 1943.6 | $1943.7 \pm 0.4$ | 1799.5 | — | $1619.4 \pm 0.2$ | 1395.6 | 1287.2 | — |

## 5. Relative intensities of the harmonic lines

All the measured intensity ratios are presented in table 6. These results are from measurements over several crystals and have not been rounded off. However, given the variation from sample to sample, their uncertainty would be about 5%.

**Table 6.** Measured intensity ratios at 10 K of the fundamental ($\nu = 1$) to the second-harmonic line ($\nu = 2$), of the higher-energy third-harmonic line ($\nu_1 = 3$) to the second-harmonic line ($\nu = 2$) and of the higher-energy third-harmonic line ($\nu_1 = 3$) to the lower-energy third-harmonic line ($\nu_2 = 3$) for H⁻ and D⁻ ions in the alkaline-earth fluorides.

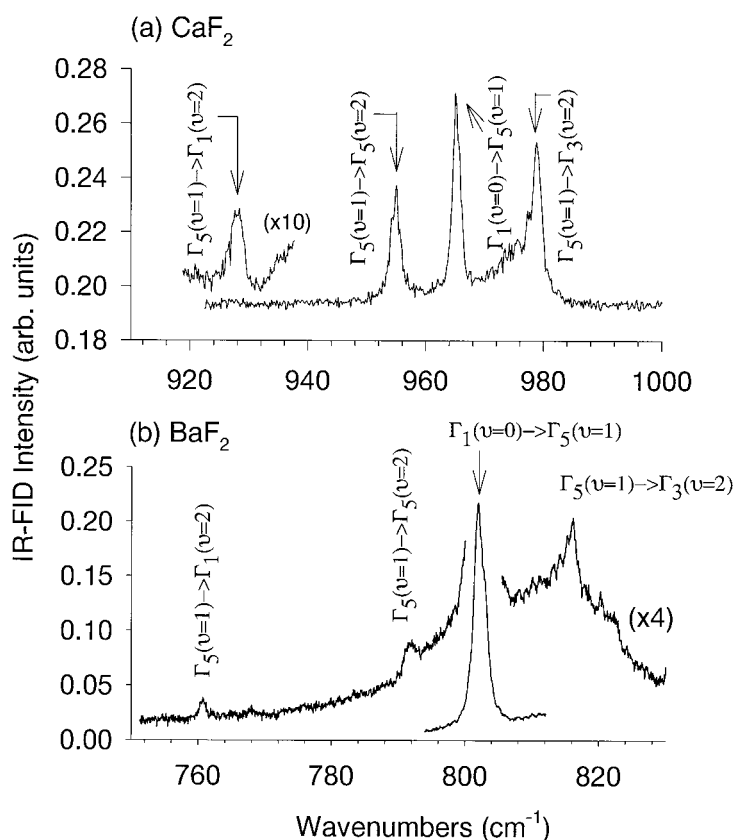| | | H⁻ | | | D⁻ | |
|---|---|---|---|---|---|---|
| Intensity ratio | $CaF_2$ | $SrF_2$ | $BaF_2$ | $CaF_2$ | $SrF_2$ | $BaF_2$ |
| $\nu = 1/\nu = 2$ | 44 | 48 | 30 | 85 | 100 | 69 |
| $\nu = 2/\nu_1 = 3$ | 61 | 48 | 41 | 44 | 75 | 57 |
| $\nu_1 = 3/\nu_2 = 3$ | 6.4 | 2.9 | 1.8 | 5.3 | 3.8 | 1.9 |

**Figure 1.** Spectroscopically resolved infrared free-induction decay exciting the fundamental local mode vibration with a time delay of 4 ps for (a) CaF$_2$ and (b) BaF$_2$. The $n = 2$ local mode levels are labelled by their appropriate T$_d$ group $\Gamma$ irreps.

As discussed in [1] for H$^-$ in CaF$_2$, the observed relative intensity of the second-harmonic line to the fundamental is substantially larger than estimated from the tetrahedral anharmonic potential model and it was necessary to introduce other processes to account for the observed intensity ratio.

SrF$_2$ and BaF$_2$ give comparable results, with SrF$_2$ having the most rapid decrease in the intensities of harmonic lines along the $\nu$ harmonic sequence.

The relative intensity ratio of the two third-harmonic lines is determined by the ratio $6C_1^2/C_2^2$ for the two quartic anharmonic constants $C_1$ and $C_2$. The revised values of these quartic anharmonic constants for H$^-$ in CaF$_2$ account well for the observed ratios. It was the good agreement obtained for the relative intensity of the two third-harmonic lines of H$^-$ for SrF$_2$ that encouraged a reassessment of these H$^-$ lines for CaF$_2$.

## 6. Observation of a fourth-harmonic line for H$^-$ in CaF$_2$

Repeated measurements for different sets of heavily hydrogenated CaF$_2$ crystals revealed the consistent presence of a weak line at 3740.0 cm$^{-1}$ of 3 cm$^{-1}$ width. Its intensity relative to the lower-frequency H$^-$ third-harmonic line is a factor of about 26 times less.

For $H^-$ in $CaF_2$, the anharmonic constants of table 3 predict the two fourth-harmonic lines to occur at 3742.3 and 3831.8 $cm^{-1}$. The lower line is in good agreement with the line observed here, while no trace of any $H^-$ line near 3831.8 $cm^{-1}$ could be observed.

## 7. Temperature dependence of linewidths of the $H^-$ and $D^-$ lines

For all three hosts, the $H^-$ fundamentals have narrow residual linewidths of less than 0.3 $cm^{-1}$ at 10 K, while the second-harmonic lines are about twice as wide. For $H^-$, the lower-frequency third-harmonic lines are all narrow with residual widths down to 0.5 $cm^{-1}$, comparable to those of the $H^-$ second harmonics. The higher-frequency third-harmonic lines have residual widths of 2.9 $cm^{-1}$ for $CaF_2$, 4.3 $cm^{-1}$ for $SrF_2$ and 7.5 $cm^{-1}$ for $BaF_2$.

All the $D^-$ lines are relatively broad. The residual linewidths at low temperatures are due to spontaneous decay of the local mode into band modes. These widths are greater for $D^-$ than for $H^-$ since the former arise from decay into two band modes, while the latter requires at least three band modes [1].

The processes governing the temperature-dependent widths have been discussed in [1]. The temperature-dependent width of the fundamental and second-harmonic lines is attributed to phonon scattering processes involving two band modes giving a $T^2$-dependence at high temperature, as observed [1]. The two third-harmonic lines form exceptions in showing broadening through processes in which band phonons cause transitions between them, as detailed in [1].

Figure 2 shows the temperature dependence of the $H^-$ third harmonics for all three hosts over the 10–110 K range where the third-harmonic lines broaden more rapidly than either the corresponding fundamental or second-harmonic lines. Furthermore, the successively broader upper third-harmonic lines along the $CaF_2$-to-$BaF_2$ sequence show successively more rapid increases in their linewidths with temperature. Both aspects indicate the rapid onset of one-phonon absorption processes, especially for $BaF_2$:$H^-$.
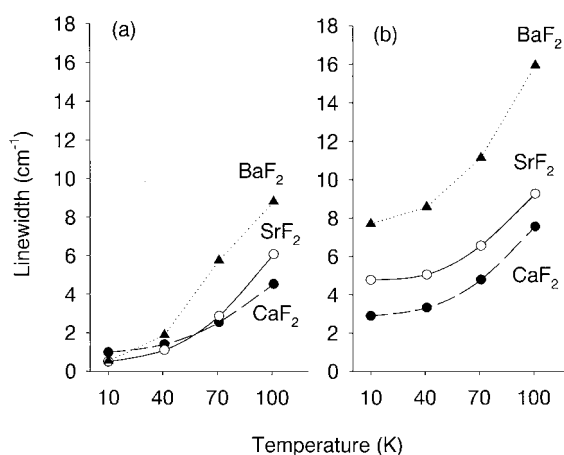


**Figure 2.** Measured linewidths of the $H^-$ third-harmonic lines as functions of temperature for (a) the lower-energy lines for $CaF_2$ (●), $SrF_2$ (○) and $BaF_2$ (▲) and (b) the corresponding higher-energy lines.

For all three hosts, the two $H^-$ third-harmonic lines are separated by an interval of about 90 $cm^{-1}$. Likewise, the two other unobserved third-harmonic levels occur at intervals of about 40 $cm^{-1}$ and 65 $cm^{-1}$ above the lowest third-harmonic level (table 4).

The higher third-harmonic lines are broadened by one-phonon emission to the lower $\nu = 3$ levels. According to equation (7-32) of [1], the one-phonon rates vary as high inverse powers of both $\Omega$ and $\omega_m$ and the increasing residual widths of the higher third-harmonic levels along the CaF$_2$-to-BaF$_2$ sequence is qualitatively understood.

The two D$^-$ third-harmonic lines are separated by an interval of about 47 cm$^{-1}$ for all three hosts. Both third-harmonic lines are broad at low temperatures through two-phonon anharmonic decay to $\nu = 2$ levels, with the lower-energy third-harmonic lines unexpectedly yet consistently broader than the higher-energy third-harmonic D$^-$ lines, especially for CaF$_2$ (table 1).

Two-phonon anharmonic decay accounts for the residual linewidths at low temperatures, but has only a weak dependence on temperature. Both D$^-$ third-harmonic lines show temperature broadening of their widths from elastic phonon scattering processes involving band modes. In contrast to the H$^-$ third harmonics, contributions from one-phonon processes appear minor for temperature broadening of the D$^-$ third harmonics.

## Acknowledgments

## References

[1] Elliott R J, Hayes W, Jones G D, Macdonald H F and Sennett C T 1965 *Proc. R. Soc.* A **289** 1–33
[2] Jones G D, Peled S, Rosenwaks S and Yatsiv S 1969 *Phys. Rev.* **183** 353–68
[3] Newman R C 1969 *Adv. Phys.* **18** 545–663
[4] Timans J W J and Den Hartog H W 1976 *Phys. Status Solidi* b **78** 283–92
[5] Jones G D and Strickland N M 1998 *Phys. Rev.* B **57** 13 471–6
[6] Strickland N M and Jones G D 2000 *Phys. Rev.* B **61** 9399–413
[7] Cockroft N J, Thompson D, Jones G D and Syme R W G 1987 *J. Chem. Phys.* **86** 521–44
[8] Reeves R J, Jones G D and Syme R W G 1989 *Phys. Rev.* B **40** 6475–84
[9] Han T P J, Jones G D and Syme R W G 1993 *Phys. Rev.* B **47** 14 706–23
[10] Tallant D R and Wright J C 1975 *J. Chem. Phys.* **63** 2074–85
[11] Cockroft N J, Han T P J, Reeves R J, Jones G D and Syme R W G 1987 *Opt. Lett.* **12** 36–8
[12] Murdoch K M and Jones G D 1998 *Phys. Rev.* B **58** 12 020–37
[13] Lee L C and Faust W L 1971 *Phys. Rev. Lett.* **26** 648–52
[14] Lang P T, Knott W J, Werling U, Renk K F, Campbell J A and Jones G D 1991 *Phys. Rev.* B **44** 6780–4
[15] Davison C P, Campbell J A, Engholm J R, Schwettman H A and Happek U 1998 *J. Lumin.* **76+77** 628–31
[16] Wells J-P R, Rella C W, Bradley I V, Galbraith I and Pidgeon C R 2000 *Phys. Rev. Lett.* **84** 4998–5001
[17] Hall J C and Schumacher R T 1962 *Phys. Rev.* **127** 1892–912
[18] Hayes W and Macdonald H F 1967 *Proc. R. Soc.* A **297** 503–19
[19] Harrington J A, Harley R T and Walker C T 1970 *Solid State Commun.* **8** 407–11
[20] Freeth C A 1989 *J. Phys.: Condens. Matter* **1** 9077–84